Assessment of the Accuracy of Gust Response Calculations by Comparison with Experiments

C. G. B. MITCHELL*
Royal Aircraft Establishment, Farnborough, Hampshire, England

Gust response calculations form part of the design process for modern aircraft, yet few comparisons of the results of calculations and flight measurements have been published. This paper describes three such comparisons, two for fighter aircraft and one for a jet transport. The gust velocity and aircraft response was measured in one of these studies, and the aircraft response only in the other two. Bending moments/g were estimated to 12% accuracy, but rms accelerations at the extremities of the aircraft, relative to that at the center of gravity, were lower in flight than had been predicted. Results also are given from model tests in which pressures on a slender delta passing through a large discrete gust were measured. Equipment is described which will enable the response of slender-wing aircraft models to large gusts to be measured.

Nomenclature

$[A]$ = inertia matrix
$[B]$ = structural damping matrix
b = span
b_n = span at transducer n
$[C]$ = structural stiffness matrix
$e(t)$ = general excitation
$f(x,y,z)$ = mode shape
$F_{jk}(\nu)$ = generalized air force in mode j due to harmonic motion in mode $k = F'_{jk}(\nu) + iF''_{jk}(\nu)$
$F_j(\nu)$ = generalized airforce in mode j due to harmonic gusts $= \mathfrak{F}'_j(\nu) + i\mathfrak{F}''_j(\nu)$
l = reference length
$m(x,y,z)$ = local element of mass
N_0 = frequency of zero crossings
$p_n(t)$ = pressure at transducer n due to a gust
q = generalized coordinate
$r(t)$ = general response
$r_1(t)$ = transient response to a unit step gust
s = distance parameter
S = area
t = time
T_r = transfer function for some response r to harmonic gusts
V = flight speed
w = gust velocity
x,y,z = coordinates
Z = displacement
$\delta(\omega)$ = Dirac delta
η = fraction of semispan
ν = frequency parameter
σ = rms
τ = time
Φ = spectral density
ω = angular frequency

Subscript

j,k = mode identification

Presented as Paper 68-892 at the AIAA Guidance, Control, and Flight Dynamics Conference, Pasadena, Calif., August 12–14, 1968; submitted August 29, 1968; revision received September 2, 1969. The author wishes to thank the Ministry of Technology for permission to present this paper, which is British Crown Copyright, and is reproduced with the permission of the Controller, Her Britannic Majesty's Stationery Office. The author would also like to thank the Office National d'Etudes et de Recherches Aerospatiales for permission to use the results of their flight measurements for Mirage III B, and the staff of both the British Aircraft Corporation (Operating) Ltd. and Hawker Siddeley Aviation Ltd. for assistance during the calculation of the responses of the P1a and Trident.

* Principal Scientific Office, Structures Department.

1. Introduction

INCREASINGLY complex automatic flight control systems are being fitted to aircraft. These systems are capable of operating at the frequencies at which the aircraft structure vibrates, and will modify the vibration characteristics of the aircraft. This modification may be undesirable, possibly causing an instability akin to flutter. Alternatively, the control system can be made to interact with the flexible airframe in a desirable manner, to improve ride comfort and reduce fatigue damage during flight in atmospheric turbulence.

Before designing a control system as a gust alleviator, it is useful to know how accurately the gust response of flexible aircraft can be predicted by present methods. It is now a routine part of the design process to make gust response calculations that include the effects of unsteady airforces, of the autopilot and autostabilizers, and of the flexibility of the structure as represented by many vibration modes.[1] However, the only comparisons between calculations of this type and flight measurements on swept or delta-wing aircraft that have been published are for the symmetric response of the B-47 to random turbulence over the frequency range 0–2 Hz,[2] for the B-47 symmetric response to discrete gusts,[3] and for the symmetric response of a nominally rigid F-106 delta-wing fighter at low supersonic speeds.[4]

This paper describes some recent work at the Royal Aircraft Establishment, Farnborough, in which the symmetric and antisymmetric responses of advanced flexible aircraft to atmospheric gusts are being studied. This is aimed at assessing the accuracy of present gust response calculation methods, first, for swept-wing flexible aircraft, by comparison with flight tests on heavily instrumented aircraft; and secondly for slender-wing flexible aircraft encountering very large gusts, by comparison with model tests in which instrumented rigid and flexible models are flown through simulated vertical gusts on a rocket-driven sledge. The results of these comparisons indicate the reliability of the calculation methods employed, and have relevance in the fields of airworthiness and in the analytical investigation of various gust alleviation concepts, with particular reference to their application to supersonic transport aircraft.

The results given here include comparisons between the calculated and measured response to turbulence of a Lightning fighter aircraft (with a 60° swept-wing) flying at $M = 0.835$ at low level; of a Mirage III fighter (60° delta-wing) flying at $M = 0.80$ at low level; and of a Trident (35° swept-wing tri-jet transport) flying at cruise speed at 15,000 ft. The slender-wing response programs are not yet complete, but results are given for the measured pressure histories on the upper surface of a sharp-edge 73° delta-wing entering a gust that increased the incidence to 13°. The experimental equipment for measuring the response of a flexible model to this same gust also is described.

2. Gust Response Calculation

2.1 Mathematical Model of the Aircraft

All the calculations described in this paper have been made by a similar method, in which the responses of the aircraft both to continuous random turbulence and to discrete gusts are calculated simultaneously. Although the particular method used to solve the equation of motion is not yet in wide use, the completeness of the description of the aircraft in these calculations does not differ significantly from that used in industrial design calculations, and the quality of the comparisons with test results reported here should be typical of that obtainable from design calculations.

The mathematical model of the aircraft is set up using normal vibration modes to represent the flexibility of the airframe. These modes, which may be calculated or based on ground resonance test measurements, are described by their normalized shapes $f_j(x,y,z)$, their natural angular frequencies ω_j rad/sec, and their generalized inertias $A_{jk} = \int m(x,y,z)\, f_j(x,y,z)\, f_k(x,y,z)\, dS$. Each mode also has some amount of structural damping.

The airforces on the wing and tail are calculated separately using Davies lifting-surface theory.[5] This is a numerical solution of the linearized integral equation connecting the unsteady pressure distribution on an harmonically oscillating wing of general planform with the downwash at chosen points on the wing, which has been programed for the ICL Mercury and Atlas computers.

In the calculations described here the lifting surface program is run for between 5 and 10 values of the frequency parameter $\nu (= \omega l/V$, where l is a typical length and V is the flight speed). The generalized airforce in each rigid and elastic mode is calculated for the pressure distributions due to harmonic oscillation in each of the rigid and elastic modes, and for those due to a pair of modes which, when added out of phase, produce a harmonic wave of downwash, equivalent to a gust, convecting over the aircraft at the flight speed.[6]

The forces due to this harmonic gust reflect the gradual penetration of the gust by the aircraft, and the delay in the development of the forces due to unsteady aerodynamic effects. Both the forces due to motion in the rigid and elastic modes of the aircraft (the response forces), and those due to the gust, are harmonic, at the frequency of the aircraft oscillation or gust, and have a frequency-dependent amplitude and phase. This frequency dependence reflects the effects that, in the time domain, lead to the gradual development of forces after a sudden change of incidence or sudden gust entry. The gust is assumed to be uniform across the span of the aircraft, and to vary only along its length.

In symmetric calculations the pressure distribution on the tailplane due to the rigid heave (vertical translation) and pitch modes are scaled by the zero frequency value of $(1 - d\epsilon/d\alpha)$ to allow for downwash at the tail, and the wing and tail forces added to give the total on the aircraft. The zero frequency values of the rigid body forces are compared with wind-tunnel measurements, and forces on the fuselage added to achieve correct values of the lift curve slope and the static margin. Fuselage contributions to the generalized airforces in the elastic modes are not included.

In lateral calculations, the airforces in the elastic modes are obtained from lifting-surface calculations, whereas the airforces in the rigid modes are obtained either from wind-tunnel tests or from lifting-surface calculations. These calculations have so far taken all the excitation of the aircraft to be due to side gusts, and have neglected the antisymmetric effects of variation of vertical gusts across the span.

For the calculations described in this paper the control surfaces have been taken to be fixed, but other calculations have been made in which movements of the control surfaces have been linked to the response of the structure at a sensor location through a complex transfer function.

2.2 Basic Solution of the Equation of Motion

The aircraft is considered to be flying through continuous harmonic gusts of wavelength λ, which force it to respond harmonically at a frequency ω rad/sec $(= 2\pi\ V/\lambda)$. The corresponding value of the frequency parameter, which determines the airforces, is ν. The aircraft is analyzed as a linear system, and the equation of motion for the harmonic response of the generalized coordinates, which represent the rigid and elastic modes, is derived from Lagranges equation. These responses are assumed small, and the forward speed of the aircraft is held constant. The axes used are typical of most flutter analyses, in that they translate along the undisturbed flight path, without rotation, at the steady flight speed.

Then, if the amplitude of the continuous harmonic gusts is w, the equation of motion for the generalized coordinates $q_j(\nu)$ can be written as

$$(-\nu^2[A] + i\nu[B] + [C] + [F'(\nu)] + i[F''(\nu)]) \times \{q(\nu)\} = w/V\{[\mathfrak{F}'(\nu)] + i[\mathfrak{F}''(\nu)]\} \quad (1)$$

where $[A]$, $[B]$, and $[C]$ are square matrices of generalized inertia, structural damping, and stiffness; $[F'(\nu)]$ and $[F''(\nu)]$ are the in-phase and quadrature coefficients of the response airforces; $\{\mathfrak{F}'(\nu)\}$ and $\{\mathfrak{F}''(\nu)\}$ are the in-phase and quadrature coefficients of the gust airforces. $\{q(\nu)\}$ is a column matrix of generalized coordinates, so that the displacement Z of a point (x,y,z) on the airframe in mode j is

$$Z(t) = l f_j(x,y,z) q_j(\nu) e^{i\nu s} \quad (2)$$

where $s\ (= Vt/l)$ is the nondimensional time or distance parameter.

It is usually more convenient to work in terms of the transfer function of the generalized coordinates $\{T_q(\nu)\}$, given by the equation

$$\{T_q(\nu)\} = (-\nu^2[A] + i\nu[B] + [C] + [F'(\nu)] + i[F''(\nu)])^{-1}(\{F'(\nu)\} + i\{\mathfrak{F}''(\nu)\}) \quad (3)$$

This transfer function is required at a large number of values of the frequency parameter ν, whereas the airforces have only been calculated at a small number of values of ν. In the course of evaluating Eq. (3), a polynomial curve is fitted to each set of values of each airforce $F_{jk}(\nu)$ or $\mathfrak{F}_j(\nu)$, and the value interpolated for the frequency at which the transfer function is being evaluated. The characteristic matrix for the aircraft is then inverted by a standard Gaussian elimination process.

After the transfer function matrix for the generalized coordinates is known to the highest frequency that is of interest, the response of the aircraft to a step gust can be calculated from the harmonic response by a Fourier transform technique.[7] If the response to a unit step gust is $\{q(s)\}$, then this is given by the integral equation

$$\{\bar{q}(s)\} = \frac{1}{2\pi}\int_{-\infty}^{\infty} \{T_q(\nu)\} \frac{e^{i\nu s}}{\nu}\, d\nu \quad (4)$$

or

$$\{\bar{q}(s)\} = \frac{2}{\pi}\int_0^\infty \tau m\{T_q(\nu)\}\ \frac{\cos\nu s}{\nu}\ d\nu \qquad (5a)$$

$$\{\bar{q}(s)\} = 2\int_0^\infty Re\{T_q(\nu)\}\ \frac{\sin\nu s}{\nu}\ d\nu \qquad (5b)$$

Equations (5a) and (5b) follow from (4) because, first, there is no response before the gust is encountered at $s = 0$, and secondly, because of the symmetry and antisymmetry of the real and imaginary parts of the transfer function. This method, and the way it has been programed for the ICL Mercury and Atlas computers, is described in more detail in the Appendix to this paper.

2.3 Response to Continuous Turbulence

Transfer functions for deflections, velocities, and accelerations of points on the structure are determined from the generalized coordinates by the use of a weighting matrix of modal deflections $[f(x,y,z)]$, so that the displacements Z at points (x,y,z) are given by

$$\{T_{Z(x,y,z)}(\omega)\} = l[f(x,y,z)]\{T_q(\nu)\} \qquad (6)$$

Structural loads are calculated by determining separately the contribution to the loads from the gust airforce, the response airforce, and the inertia loads, and adding these. This appears to be a more reliable method than the alternative, in which the structural loads are estimated directly from the local mode shapes.

Finally, the random response of the aircraft to continuous random turbulence is calculated by a standard application of the power spectral density approach. For excitation by turbulence with a spectral density $\Phi(\omega)$, the spectral density of some response quantity $\Phi_{rr}(\omega)$ is given by

$$\Phi_{rr}(\omega) = |T_r(\omega)|^2\Phi(\omega) \qquad (7)$$

where $T_r(\omega)$ is the transfer function describing the response to harmonic gusts. The rms of the response σ_r is found by integrating the spectrum of the response

$$\sigma_r^2 = \int_0^\infty \Phi_{rr}(\omega)d\omega \qquad (8)$$

If the excitation and its first derivative are independent and each has a Gaussian probability distribution, then the frequency of zero crossings with a positive slope is

$$N_0 = \frac{1}{2\pi\sigma_r}\left[\int_0^\infty \Phi_{rr}(\omega)\omega^2 d\omega\right]^{1/2} \qquad (9)$$

Both the integrals in Eqs. (8) and (9) should cover the frequency range zero to infinity. In practice, the integration may have to be stopped at some high frequency in calculations and flight measurements, and at some low frequency in measurements. The resulting values of σ and N_0 are called "truncated." Throughout the work described in this paper, great care has been taken to ensure that when the results of flight measurements and calculations are compared, the experimental and theoretical spectra are integrated over the same frequency range.

2.4 Response to Discrete Gusts

The histories of the displacements, velocities, and accelerations of points on the structure are calculated from the corresponding responses of the generalized coordinates in a step gust, by the use of a weighting matrix as in Eq. (6). The histories of the structural loads are found from their transfer functions by the Fourier transform method described before.

Once the response to a step gust $r_1(t)$ is known, the response $r(t)$ to a general gust $w(t)$ is found by the use of Duhamel's superposition integral.

$$r(t) = r_1(t)w(0) + \int_0^t r_1(t-\tau)\frac{dw}{dt}(\tau)d\tau \qquad (10)$$

3. Application to Specific Aircraft with Flight Test Comparisons

3.1 General

There are many ways of comparing the calculated and measured responses of an aircraft to atmospheric turbulence. If the turbulence encountered during the experimental flying was measured, both the magnitudes and phases of the transfer functions of interesting response quantities can be determined from the measurements, and compared directly with the calculated transfer functions. This was done in Ref. (2) for the B-47 and has been done for some measurements that have been made on an MS-760 straight-wing jet trainer at the College of Aeronautics, Cranfield.[14]

In cases where the turbulence encountered was not measured it has to be estimated, and this can introduce errors. The experimental spectra can be divided by the estimated turbulence spectrum to provide estimates of the magnitudes of the transfer functions. Alternatively, the calculated transfer functions can be multiplied by the estimated turbulence spectrum to provide response spectra, for comparison with the measurements.

The comparisons described previously are essentially qualitative, in that the shapes of the spectra or transfer functions are compared. Some degree of quantitative assessment of the comparison can be made by determining the frequencies and dampings of major response peaks.

Comparisons that are perhaps more directly relevant to the engineering use of response spectra are of the rms response to a unit rms gust, the ratios of the rms of the various response quantities, and the frequencies of zero crossings of the responses. All these types of comparisons are used during the remainder of this paper. The three flight measurement programs which provided the data for these comparisons were not undertaken primarily for that purpose, and unfortunately the gust velocity was only measured during one of the three. For the other two investigations it was, therefore, not possible to compare the measured and calculated aircraft responses per unit rms gust, and so in these cases the responses were normalized with respect to the normal acceleration near the center of gravity of the aircraft.

3.2 Lightning Fighter

In 1959, the response of the second prototype P1a Lightning fighter was measured during flight at $M = 0.835$ at 1000 ft through atmospheric turbulence.[8] The aircraft, which has a 60° swept wing and a delta tailplane, was instrumented with ten accelerometers (six normal and four lateral) and three rate gyros, as is shown in Fig. 1. Records of accelerations and angular rates were made on photographic paper during a number of runs in turbulence. These were analyzed to provide spectral densities of the aircraft responses for the frequency range 0.45 to 15 Hz for the normal and lateral accelerations near the cg, and the angular rates, and for the range 1 to 30 Hz for the remaining accelerations. The gust velocities were not measured.

The test aircraft was subsequently resonance tested and its response to vertical and lateral gusts calculated separately.[9] The calculations included the two symmetric and three antisymmetric rigid body modes, five symmetric elastic modes with frequencies between 6 and 37 Hz, and four antisymmetric modes with frequencies between 9 and 17 Hz. Measurement of several of these modes on the ground had proved

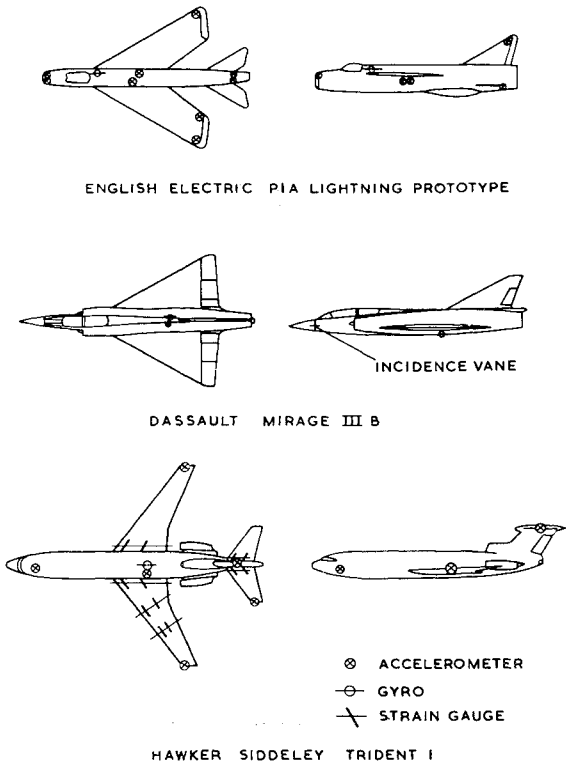

Fig. 1 Test aircraft and instrumentation positions.

difficult, as at some frequencies the aircraft vibrated asymmetrically and with large phase differences between the motion of the wings and the tail.

When the wing and tail symmetric airforces were calculated it was found that $dC_L/d\alpha$ and the static margin agreed with test values to 3% and to 0.3% root chord, respectively, so fuselage airforces were not included in the symmetric calculation.

As the turbulence encountered during the flight tests was not measured, it was assumed to have a spectrum similar to that measured on another occasion in the same area, at the same height and at the same time of year. This spectrum was used to allow an estimate to be made of the transfer function for the c.g. normal acceleration from the flight measurements, and also to enable the spectral densities of all the response accelerations to be predicted. Vertical and lateral gusts were taken to be uncorrelated, and to have the same rms intensity and scale.

In Fig. 2 are shown the calculated and measured transfer functions for the c.g. normal acceleration. The measured function is the average of 17 estimates deduced from separate test runs, with its amplitude scaled to coincide with the calculated function at 2 Hz, where variation with frequency is small.

Figure 3 shows the calculated and measured spectra for the normal and lateral c.g. acceleration, and the accelerations

Table 1 Normalized rms accelerations for lightning

Acceleration	Calculated	Measured
c.g. normal	1.00	1.00
c.g. lateral	0.26	0.25
Front fuselage normal	0.91	0.78
Front fuselage lateral	0.53	0.35
Rear fuselage normal	1.50	1.06
Rear fuselage lateral	0.88	0.38
Port wing tip normal	3.29	2.52
Stbd wing tip normal		2.41
Aileron root normal	2.64	1.95
Fin tip lateral	7.53	2.68

at the wing and fin tips. The calculated values are in turbulence with an rms velocity of 1 m/sec, whereas the measured values are from a 40-sec run in turbulence of unknown velocity. Comparison of the two suggests that the test turbulence had an rms of approximately 1.5 m/sec.

The symmetric response calculation gave generally better results than the antisymmetric. The short period mode was well predicted, and differed only slightly between rigid and flexible aircraft calculations. The dutch roll mode was predicted rather badly by the rigid aircraft calculation, but inclusion of the airframe flexibility improved the agreement with the measurements considerably. Accuracy of the prediction of the structural accelerations decreased as the frequency was raised and also as the point at which the acceleration was measured was moved toward the extremities of the aircraft. The calculated and measured rms accelerations, normalized with respect to the c.g. normal acceleration, are listed in Table 1.

The conclusions of Ref. 9 were 1) calculations in which the gust velocity is assumed constant across the span tend to overestimate the accelerations of the extremities of the aircraft, particularly at high frequency; 2) impurity of vibration modes measured during resonance tests can lead to appreciable errors in the response calculations; and 3) to obtain statistically reliable results from flight tests, it is necessary to make long test runs, or a number of runs, in turbulence under nominally identical conditions.

3.3 Mirage III

A further comparison of the response of a fighter aircraft to low-altitude turbulence has been made in cooperation with the French Office National d'Etudes et de Recherches Aerospatiales (ONERA).[10] In this, ONERA was wholly responsible for all aspects of the experimental work and for the analysis of the flight measurements. The aircraft in this instance was a Mirage III B fighter with a 60° delta wing, which was flown at $M = 0.80$ at low level along the Mediterranean coast. Two test runs were made, each lasting about 10 min. The aircraft was fitted with an incidence vane, a normal accelerometer near the c.g., a pitch gyro and a control transducer (see Fig. 1). Analogue measurements from these instruments were recorded continuously on mag-

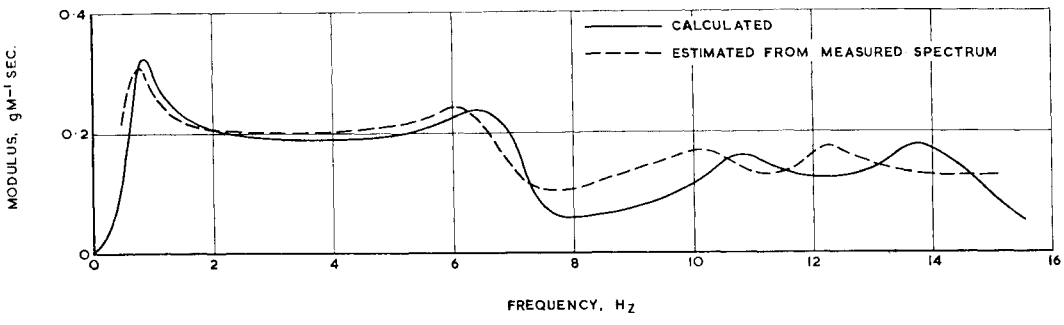

Fig. 2 Transfer function for lightning normal acceleration of the structure near the c.g.

netic tape, and were analyzed, using an analogue computer, to provide transfer functions for the normal acceleration and pitch rate due to turbulence, the spectrum of the vertical gust velocity, and the frequencies of level crossings for the gust velocity, e.g. acceleration and pitch rate.

The transfer function for the normal acceleration near the c.g. was calculated for the flexible aircraft. Flexibility was represented by two measured normal modes at 10.5 and 13.6 Hz. As the weight and position of the center of gravity varied appreciably during the measurement runs, the calculation was made for average values of these parameters. Figure 4 shows the calculated transfer function, together with experimental points from the flight measurements.

Because of its stiffness, little could be learned of the dynamic effects of structural flexibility on the response of the aircraft to turbulence. The flexibility introduced by the two modes had a detectable effect on the short period motion. The main value of this experiment was to confirm the ability of present methods to calculate the absolute values of transfer functions for aircraft in turbulence.

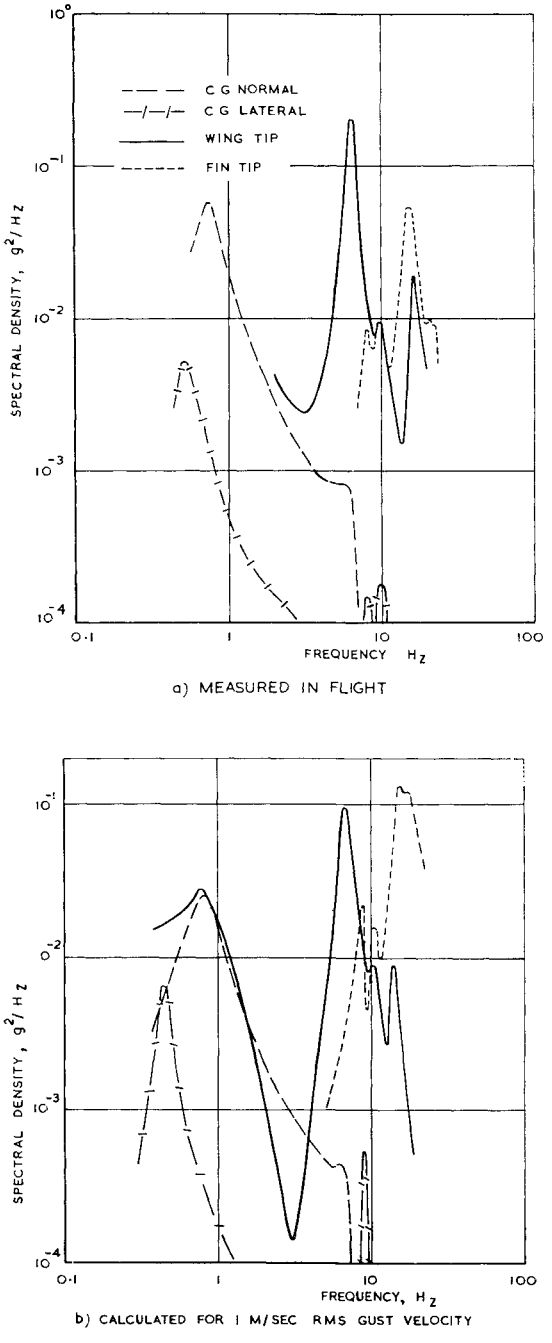

Fig. 3 Spectra for lightning accelerations.

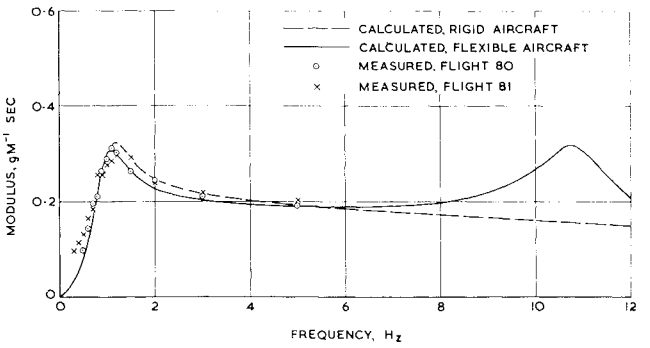

Fig. 4 Transfer function for Mirage III acceleration of the structure near the c.g.

3.4 Trident

An extension of the response study made on the Lightning fighter was started in 1966, when a specially instrumented H.S. Trident series 1 tri-jet transport with a 35° swept wing and a T-tail was flown in turbulence at $M = 0.55$ at 15,000 ft (268 kt eas).[11] A number of symmetric and antisymmetric response accelerations and structural strains were measured, the instrument layout for the symmetric response quantities being shown in Fig. 1. Measurement runs were made with the autopilot engaged, with the autopilot off but the roll and yaw dampers operating, and with the autopilot and dampers off. The response quantities were recorded on magnetic tape, and were later digitized and analyzed to provide spectral densities for the frequency range 0.2–12 Hz.

Calculations were made[12] for the symmetric response of the aircraft to random turbulence with a spectral density given by

$$\Phi(\omega) = \frac{L}{\pi V} \frac{1 + \frac{8}{3}(1.339\ \omega L/V)^2}{[1 + (1.339\ \omega L/V)^2]^{11/6}} \qquad (11)$$

where L, the scale length, was taken to be 2500 ft. Further calculations with scales between 250 and 5000 ft were made to assess the importance of this parameter.

The aircraft flexibility was represented by 6 calculated normal modes with frequencies in the range 2.8–15.5 Hz. Bending moments at three wing stations and one tailplane station were calculated by determining separately the contribution to these from the gust airforces, the response airforces, and the inertia forces. The wing bending moments caused by turbulence and by slow sinusoidal maneuvers were calculated, and the ratio of the $(BM/g)_{gust}$ to the (BM/g) maneuver defined as the turbulence response factor. Since the wing strain gages were calibrated in flight by making slow pull-up maneuvers, the ratio of $(strain/g)_{gust}$ to $(strain/g)$ maneuver was the quantity that was directly measured, and from which an estimate of the wing bending moments in turbulence was made.

Figure 5 shows a comparison of the calculated and measured spectra for the normal accelerations on the structure near the c.g., at the wing tip and at the centerline of the tailplane. The wing tip spectra show only the accelerations caused by symmetric modes. The difference in magnitude between the 2 sets of spectra is due to the intensity of the turbulence encountered during the flight measurement. This can be deduced to have been 2.3 m/sec tas rms velocity. The calculated and measured values of the rms accelerations, normalized by the acceleration on the structure near the c.g., are given in Table 2. As an example of the spectrum of a structural load, Fig. 6 shows the calculated and measured spectra of the tailplane bending moment.

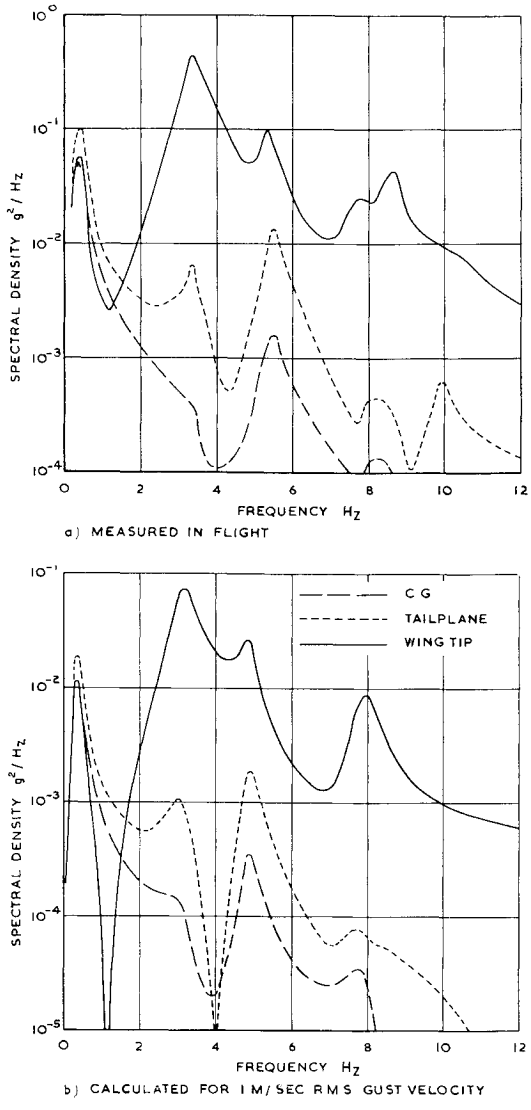

Fig. 5 Spectra for Trident accelerations.

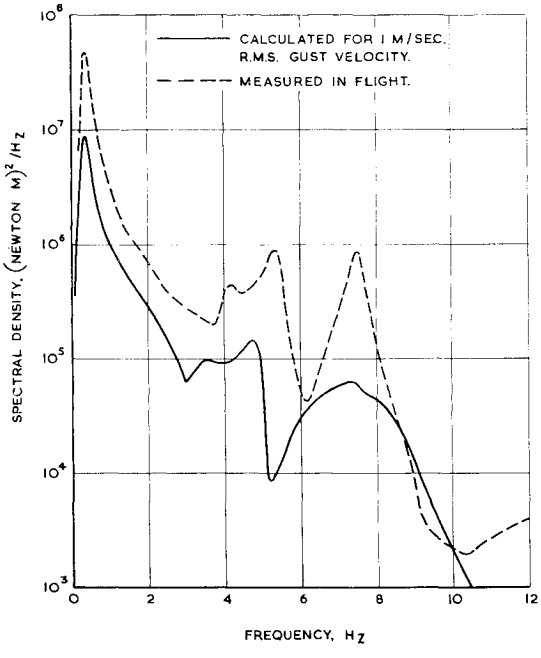

Fig. 6 Spectrum for Trident tailplane root bending moment.

Table 2 Normalized rms responses for Trident

Response	Calculated	Measured Run 19	Measured Run 20
Accelerations			
c.g. normal	1.00	1.00	1.00
Cockpit	0.91	0.70	0.77
Tailplane centerline	1.50	1.50	1.52
Wing tip	5.14	5.07	4.10
Bending moment			
Tailplane root, NM/g	31,300	28,900	28,700
$(BM/g)_{gust}/(BM/g)_{manoeuvre}$			
Wing root, $\eta = 0.17$	0.87	0.96	0.95
Wing rib 8, $\eta = 0.42$	0.91	1.03	1.01
Wing rib 13, $\eta = 0.69$	0.93	0.87	0.89

The variation along the wing of the turbulence response factor for bending moment is shown in Fig. 7, together with the frequency of zero crossings. The turbulence response factor has been calculated for continuous random turbulence and (see below) for discrete gusts, and is compared with measurements in continuous turbulence. N_0 has been calculated and measured in continuous turbulence only.

Calculations have been made for the response of the aircraft to discrete ramp gusts, in which the gust velocity increases linearly to some maximum value, which is then held steady. These calculations have been made for ramp lengths of between 0 and 300 ft, and for each ramp length the maximum values of the transient accelerations and bending moments noted, for unit gust velocity. These maximum values vary considerably with gust length, but when the ratios of the bending moments to the acceleration of the structure near the c.g. are calculated they are found to vary less as the gust ramp length is changed. The values of the 4 bending moments/g for discrete gusts are shown in Fig. 8. The turbulence response factors have been calculated by taking the average values of the BM/g for gust lengths of 0–300 ft, and dividing this by the BM/g in a maneuver.

The calculation seems to have overestimated the extent to which the elastic modes are excited by turbulence. In the case of the cockpit and tailplane accelerations, this conclusion cannot be made directly from the rms accelerations, as the calculation has under estimated the pitching of the aircraft at the short period frequency by about 10%.

Although the accelerations at the extremities of the aircraft are overestimated by the calculation, the elastic modes contribute little to the structural loads, and agreement between the calculated and measured loads and turbulence response factors is quite good. Both continuous turbulence and discrete gust calculations give results that agree with the flight measurements to within 12%, with average errors of 9% and 8%, respectively. However, along the wing the trends of the calculated and measured turbulence response factors differ, again suggesting that the calculation has overestimated the excitation of the elastic modes.

4. Model Tests to Determine the Response of Supersonic Transport Aircraft to Atmospheric Turbulence

4.1 General

During the development of Concorde, many calculations have been made to determine the response of slender-wing aircraft in general, and supersonic transports in particular, to discrete gusts and to continuous turbulence. Some of the early results were unusual, but as the aircraft has become more fully defined, and as the calculations have become more detailed, its dynamic characteristics have emerged as being typical of a moderately large, rather flexible, transport air-

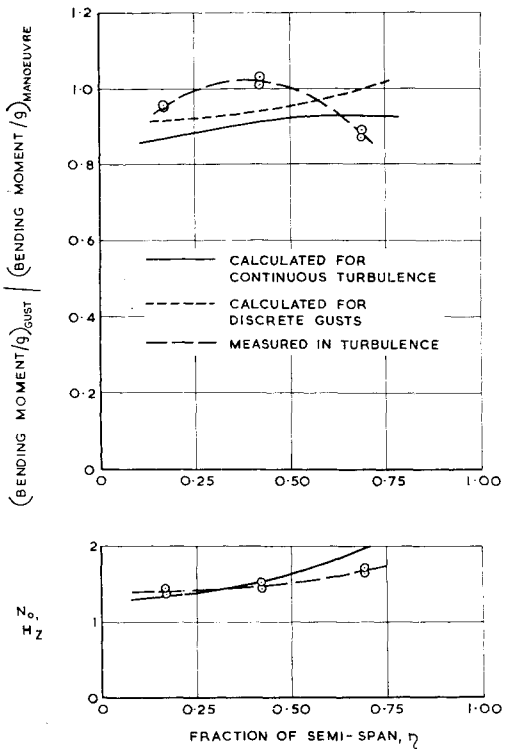

Fig. 7 Trident wing bending moments.

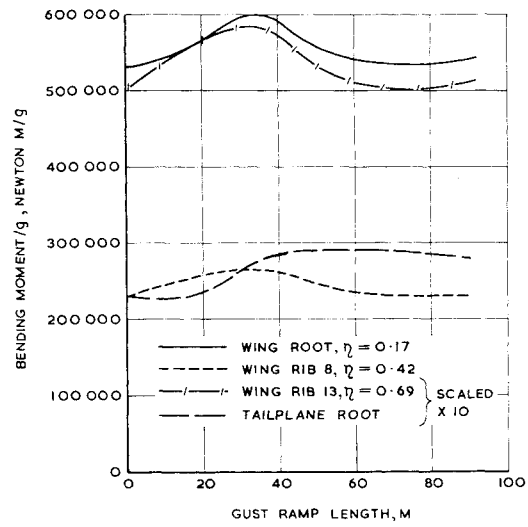

Fig. 8 Trident response to discrete gusts.

craft. However, almost all of the dynamic response calculations to date have assumed that the unsteady airforces on the flexible wing are those associated with attached flow, and that these forces can be calculated from the conventional linearized equations connecting the downwash at a wing and the pressure distribution on it.

This assumption is, of course, quite inadequate with regard to the steady airforces acting on a slender wing with sharp leading edges, from which the flow separates. However, making this assumption, it has proved possible to predict symmetric flutter speeds for slender wing models at low Mach numbers very accurately.

To determine the transient airforces on slender wings in large gusts, and to study the response of slender-wing aircraft to these gusts, two sets of model tests have been made. These are described below.†

4.2 Transient Pressures in Large Gusts

The change of pressure at four points on the upper surface of a slender-delta wing entering and leaving a large gust have been measured in a series of model tests.[13] The model, which is sketched in Fig. 9, was 30 in. long and had an aspect ratio of 1.2. It was fitted with four pressure transducers equally spaced along a ray at 0.75 semispan, the forward transducer being 9 in. and the aft transducer 18 in. aft of the apex. The model was mounted rigidly on an aerodynamically stabilized dart on a sledge that can be fired at up to 200 ft/sec along a high-speed track. The track passes an open jet wind tunnel, the efflux from which can produce a uniform gust $4\frac{1}{2}$ ft deep along a 15-ft length of the track. The gust velocity is 46 ft/sec, which causes an incidence change at the wing of about 13°. The jet that produces the gust has mixing zones about 10 in. deep at its edges.

The model was flown through the gust at initial incidences of 0, 5, and 10° and the histories of the four pressures $p_n(t)$ recorded. These histories were normalized by the final pressures $p_n(\infty)$ and plotted against a nondimensional time s' based on the local span b_n (so that $s' = Vt/b_n$). This collapsed the results from the four transducers onto a single curve. There was less scatter between the individual curves for a single run than between the mean curves for different runs. This latter variation was probably caused by differences of the velocity profile in the mixing zone at the edge of the gust.

At each of the transducers, the pressure did not change until the transducer entered the gust. After entering the gust, the normalized pressure $p_n(t)/p_n(\infty)$ had reached a value of 0.8 in the time taken by the wing to travel between $1\frac{1}{2}$ and 4 times the local span, and by the time it had traveled 5 times the local span $p_n(t)/p_n(\infty)$ was between 0.9 and 1.0. At no time did a pressure exceed its final steady value. As each transducer left the gust, the local pressure returned to its undisturbed value almost instantaneously.

The four corresponding pressure histories for the delta-wing entering a step gust were calculated assuming the flow over the wing did not separate from the leading edges. This was done by using Davies lifting-surface program to calculate the harmonic pressures, at the positions of the transducers, caused by harmonic gusts. The Fourier transform programs described in the Appendix were then used to derive the transient pressures due to a step gust. Apart from the attached flow assumption, the calculated pressures are differ-

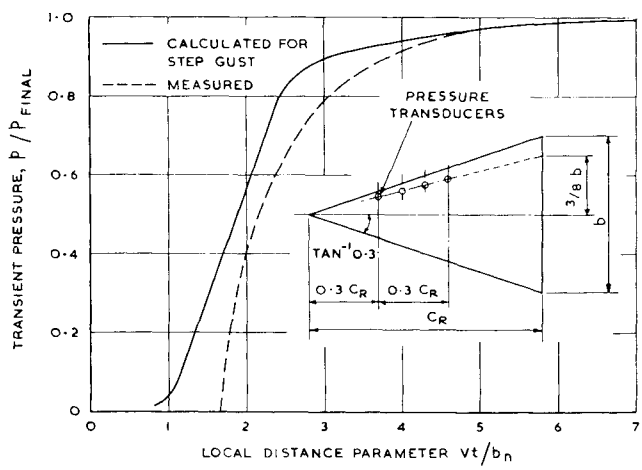

Fig. 9 The pressure rise on a slender delta entering a discrete gust.

† These experiments were made at R.A.E. Farnborough by D. R. Roberts and G. K. Hunt, and by H. Hall and R. Cansdale, respectively.

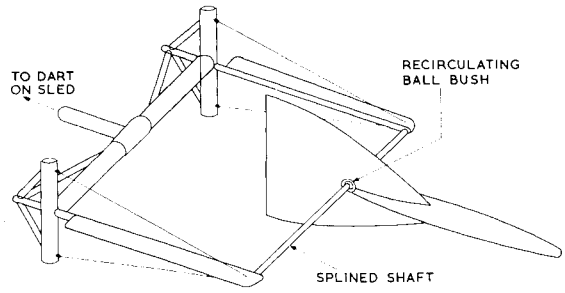

Fig. 10 Slender wing gust response model.

ential across the wing, whereas the measured pressures are for the top surface only.

The calculated pressure histories were normalized, and collapsed onto a single curve when plotted against s' ($= Vt/b_n$). This curve is compared, in Fig. 9 with the fastest-changing measured history. This fastest history was chosen as being the one appropriate to a near-step shape of gust. It will be seen that the calculated history, which would apply to both gust entry and exit if the wing aerodynamics were linear, actually agrees rather well with the measured history with separated flow. This suggests that the rate at which the forces develop on a wing is not very sensitive to the details of the flow pattern producing the forces. However, the measured pressure histories at exit from the gust bear no resemblance to the calculated, and are in practice much more abrupt.[13]

4.3 Transient Response to Large Gusts

A further series of model tests is currently being made, using the gust track facility described previously, to measure the symmetric response of rigid and flexible slender-wing models to large discrete gusts.[15] The models are mounted on a slide that allows symmetric translation and pitch, and are released from the end of the slide just before entering the gust. (Because the gust blows horizontally across the track the model is mounted rolled through 90°, and lateral motion across the track simulates symmetric, or vertical, motion of the model in model coordinates.) The model, on its slide, is carried by a dart on the sledge of the high-speed track, as is shown in Fig. 10. The rigid and flexible models are identical aerodynamically, and have an ogival wing of aspect ratio 1.2.

The rigid model, which so far has been used to develop the instrumentation system, is fitted with normal accelerometers near the c.g. and in the nose. Signals from these are recorded on a tape recorder carried on the sledge. The model is filmed also by a camera on the sledge, and by another mounted above the gust tunnel.

It has proved to be difficult to avoid contamination of the signal by the response of the model to track roughness, but this has now been done by making changes to both the model support and to the instrumentation system. Useful results are being produced and it is hoped that soon it will be possible to obtain results that are of sufficient quality to allow comparison with linear and nonlinear gust response calculations.

The flexible model is made from an aluminum alloy plate machined to provide the desired structural stiffness, ballasted to the correct mass distribution, and covered with a foamed plastic to provide a smooth aerodynamic shape. It is instrumented with 12 miniature accelerometers. It is likely that the use of this model on the gust track will cause more difficulties from signal contamination and from variation of the detailed shape of the simulated gust, but provided these can be overcome the experiment should provide a new insight into the effect of nonlinear aerodynamic forces on the gust response of flexible aircraft.

5. Discussion and Conclusions

The standard of the gust response calculations described in this paper is believed to be typical of those made to date. Improvements that can be immediately foreseen are the inclusion of the unsteady aerodynamic interference between the wing and tailplane, and the extension of the calculations to include the variation of the turbulence across the span of the aircraft. Both these improvements will increase the amount of computing significantly.

It has been shown, by comparison with flight measurements, that the present standard calculations are capable of predicting the low-frequency behavior of elastic aircraft to an accuracy of about 10%, but that they overestimate the excitation of the higher frequency elastic modes appreciably. Because most structural loading occurs at the lower frequencies, it can be estimated to within 15%. The accelerations at the extremities of flexible aircraft are lower in flight than would be predicted.

The accuracy of the flight measurements reported in this paper was probably 5 to 10% on rms values, and so was comparable to the accuracy of the calculations. Until greater accuracy is needed for design purposes, and can be obtained from flight measurements, there would appear to be little justification for elaborating the calculations, except as a research exercise to make methods available in case of need.

Because of the coincidental similarity of the attached and separated flow transient pressure histories on slender wings entering gusts, the use of linearized aerodynamic theories for some response problems on this class of aircraft appears justified. However, it must be noted that the change in pressure on these wings is almost instantaneous when they go from a lifting to a nonlifting condition. This should be represented in calculations of the response to gusts that reduce, but do not reverse, the lift on such aircraft.

Appendix: Calculation of the Response to Discrete Step Gusts by a Transform Method

For linear systems, the responses to harmonic and transient excitation are related. If the transfer function for a particular parameter is $T_{re}(\omega)$, then the transient response of that parameter $r(t)$ to transient excitation $e(t)$ is given by

$$\overline{r(\omega)} = T_{re}(\omega)\overline{e(\omega)} \tag{A1}$$

where $\overline{r(\omega)}$ and $\overline{e(\omega)}$ are the Fourier transforms of $r(t)$ and $e(t)$. These are defined as

$$\overline{r(\omega)} = \int_{-\infty}^{\infty} r(t)e^{-i\omega t}\,dt \tag{A2}$$

$$r(t) = \frac{1}{2\pi}\int_{-\infty}^{\infty} \overline{r(\omega)}e^{i\omega t}\,d\omega \tag{A3}$$

$\overline{e(\omega)}$ and $e(t)$ are similarly related.

To calculate the response of an aircraft to a discrete unit step gust, having $w = 0, t \leqslant 0$; $w = 1, t > 0$, we note that the transform of a unit step $1(t)$ is

$$\overline{1(t)} = \pi\delta(\omega) + (1/i\omega) \tag{A4}$$

Thus, the transform of the response to a unit step gust is

$$\overline{r_1(\omega)} = (T_r(\omega)/i\omega) + \pi\delta(\omega)T_r(\omega) \tag{A5}$$

where $T_r(\omega)$ is the transfer function for the response to harmonic gusts. To avoid a singularity in $\overline{r_1(\omega)}$ at $\omega = 0$, it is necessary for $T_r(\omega)$ to tend to zero as ω tends to zero, so the second term in Eq. (A5) does not, in practice, contribute to $\overline{r_1(\omega)}$.

The transform of the response has real and imaginary parts, so that

$$\overline{r_1(\omega)} = \bar{r}_1'(\omega) + i\bar{r}_1''(\omega) \quad \text{(A6)}$$

$\bar{r}'_1(\omega)$ is an even function of ω, $\bar{r}''_1(\omega)$ is an odd function, and $r_1(t) = 0$ for $t \leqslant 0$. With these conditions $r(t)$ can be evaluated independently from either $\bar{r}'_1(\omega)$ or $\bar{r}''_1(\omega)$

$$r_1(t) = \frac{2}{\pi}\int_0^\infty \bar{r}_1'(\omega)\cos\omega t\, d\omega \quad \text{(A7)}$$

$$r_1(t) = -\frac{2}{\pi}\int_0^\infty \bar{r}''_1(\omega)\sin\omega t\, d\omega \quad \text{(A8)}$$

Substitution of Eq. (A5) in Eqs. (A7) and (A8) gives the main paper Eqs. (5a) and (5b).

Equations (A7) and (A8) can be integrated to some high, but finite, value of ω. As this cut-off frequency is raised the value of the truncated integral oscillates about its true value, passing near it when $\omega t = n\pi$ for Eq. (A7) and $\omega t = \pi(2n + 1)/2$ for Eq. (A8), n being an integer. To obtain an accurate estimate of $r_1(t)$, the integral in Eq. (A7) is evaluated to a value of n, say N, that corresponds to an ω beyond which $\bar{r}'_1(\omega)$ reduces monotonically with increasing ω. This value, $r_1{}^N$, is stored and the integration continued to evaluate $r_1{}^{N+1}$. A good estimate of $r_1(t)$ is then the average of $r_1{}^N$ and $r_1{}^{N+1}$. The integral in Eq. (A8) is evaluated similarly.

These integrations are carried out numerically on a digital computer using a program that has been combined with the one that forms and solves Eq. (3) for the aircraft transfer function. This ensures that penetration of the gust and unsteady aerodynamic effects on the gust and response airforces are included in the calculation of both the harmonic and the transient responses of the aircraft in an identical manner.

References

[1] Hitch, H. P. Y., "Modern Methods of Investigating Flutter and Vibration," *Journal of the Royal Aeronautical Society*, Vol. 68, No. 642, June 1964, pp. 357–373.

[2] Bennett, F. V. and Pratt, K. G., "Calculated Responses of a Large Swept Wing Airplane to Continuous Turbulence with Flight Test Comparisons," TR R-69, 1960, NASA.

[3] Jackson, C. E. and Wherry, J. E., "A Comparison of Theoretical and Experimental Loads on the B-47 Resulting from Discrete Gusts," *Journal of Aeronautical Sciences*, Vol. 16, No. 1, Jan. 1959, pp. 33–45.

[4] Houbolt, J. C., Steiner, R., and Pratt, K. G., "Dynamic Response of Airplanes to Atmospheric Turbulence Including Flight Data on Input and Response," TR R-199, 1964, NASA.

[5] Davies, D. E., "Calculation of Unsteady Generalised Air Forces on a Thin Wing Oscillating Harmonically in Subsonic Flow," Rept. and Memo 3409 (replaces Royal Aircraft Establishment Report Structures 290, 1963), 1966, British Aeronautical Research Council.

[6] Murrow, H. N., Pratt, K. G., and Drischler, J. A., "An Application of a Numerical Technique to Lifting Surface Theory for Calculation of Unsteady Aerodynamic Forces due to Continuous Sinusoidal Gusts on Several Wing Planforms at Subsonic Speeds," TN D-1501, 1963, NASA.

[7] Mitchell, C. G. B., "Computer Programmes to Calculate the Response of Flexible Aircraft to Gusts and Control Movements," Current Paper 957 (replaces Royal Aircraft Establishment TR 66332, 1966), 1967, British Aeronautical Research Council.

[8] Burnham, J., Savory, J. M., and Mote, H. I., "Measurements of the Response of a Fighter Aeroplane to Turbulent Air and a Comparison with the Results of Ground Resonance Tests," TN Aero 2746, 1961, Royal Aircraft Establishment.

[9] Mitchell, C. G. B., "Calculation of the Response of a Fighter Aircraft to Turbulent Air and a Comparison with Flight Measurements," TR 66275, 1966, Royal Aircraft Establishment.

[10] Coupry, G., "Response du Mirage III B 225 a La Turbulence," TR (unpublished), 1966, Office National d'Etudes et Recherches Aérospatiales, 92 Chatillon, France.

[11] "Rough Air Flight Tests on a Trident," Rept. (unpublished), 1967, Hawker Siddeley Aviation Ltd., Hatfield, Herts, England.

[12] Mitchell, C. G. B., "Calculation of the Response of a Transport Aircraft to Continuous Turbulence and Discrete Gusts and a Comparison with Flight Measurements," Current Paper 1035, 1969 (replaces Royal Aircraft Establishment TR 68083, 1968), British Aeronautical Research Council.

[13] Roberts, D. R. and Hunt, G. K., "Further Measurements of Transient Pressures on a Narrow-Delta Wing due to a Vertical Gust," TR 66124, 1966, Royal Aircraft Establishment.

[14] Williams, D. A., "Measurement of the Symmetric Response of the MS 760 Paris Aircraft to Atmospheric Turbulence," Rept. Aero 211, 1969, College of Aeronautics, Cranfield, Bedford, England.

[15] Cansdale, R. and Hall, H., "Gust Response Measurements on a Model Aircraft," TR 69273, 1969, Royal Aircraft Establishment.